Journal of Statistical Mechanics: Theory and Experiment
An IOP and SISSA journal

PAPER: Quantum statistical physics, condensed matter, integrable systems

Two-point connectivity of two-dimensional critical Q-Potts random clusters on the torus

Nina Javerzat[1], **Marco Picco**[2] **and Raoul Santachiara**[1]

[1] LPTMS, CNRS (UMR 8626), Univ.Paris-Sud, Université Paris-Saclay, 91405 Orsay, France
[2] LPTHE, UMR 7589, Sorbonne Université and CNRS, France
E-mail: nina.javerzat@u-psud.fr, picco@lpthe.jussieu.fr and raoul.santachiara@u-psud.fr

Received 29 August 2019
Accepted for publication 28 November 2019
Published 4 February 2020

Online at stacks.iop.org/JSTAT/2020/023101
https://doi.org/10.1088/1742-5468/ab6331

Abstract. We consider the two dimensional Q-random-cluster Potts model on the torus and at the critical point. We study the probability for two points to be connected by a cluster for general values of $Q \in [1, 4]$. Using a conformal field theory (CFT) approach, we provide the leading topological corrections to the plane limit of this probability. These corrections have universal nature and include, as a special case, the universality class of two-dimensional critical percolation. We compare our predictions to Monte Carlo measurements. Finally, we take Monte Carlo measurements of the torus energy one-point function that we compare to CFT computations.

Keywords: conformal field theory, correlation functions

J. Stat. Mech. (2020) 023101

1742-5468/20/023101+23$33.00

Contents

1. Introduction **2**

2. Conformal field theory on a torus **3**
2.1. Virasoro algebra and its representation 3
2.2. Torus correlation functions 5

3. Q-Potts random cluster model **7**

4. Two-point Potts torus connectivity **8**
4.1. Identity channel contributions 10
4.2. Energy channel contributions 11
4.3. $(1,3)^D$ channel contributions 13

5. Monte Carlo simulation and CFT comparisons **14**
5.1. General results for the two-point correlation functions 14
5.2. Non-square torus 16
5.3. Link with one-point correlation function 16
5.4. Further corrections 18

6. Conclusions **20**
Acknowledgments **20**
Appendix. The s-channel expansion of the torus two-point function **20**

References **22**

1. Introduction

The critical point of a two-dimensional statistical model can be often characterised in terms of extended objects that, in the continuum limit, are described by conformal invariant fractal structures [1]. The study of these fractals provided new insights into the nature of critical phenomena paving the way to mathematically rigorous approaches [2]. On the one hand, many of the results found so far involve quantities related to two-point correlation functions of a conformal field theory (CFT). The only exceptions concern observables that satisfy some differential equation and whose definition requires the existence of a boundary, such as crossing probabilities [3] or SLE interfaces [4]. On the other hand, the (bootstrap) solution of a CFT requires the knowledge of three- and four-point correlation functions. Besides some special cases [5, 6], the only known bootstrap solutions known to describe statistical critical points are the minimal models. These CFTs have been successful in providing the behaviour of local observables of critical systems, such as the Ising spin correlation function, but they are too simple to capture the geometry of conformal fractals. The description of these fractals hints therefore at the existence of a CFT whose solution remains an open puzzle.

https://doi.org/10.1088/1742-5468/ab6331

J. Stat. Mech. (2020) 023101

The random cluster Q-state Potts models [7] represent an ideal laboratory in this context. This is a one parameter family of models which includes as special cases the spanning forests ($Q \to 0$) [8], the (bond) percolation ($Q = 1$), the Ising ($Q = 2$) and the three-state Potts ($Q = 3$) spin models, as well as the permutation symmetric point of the Ashkin–Teller model ($Q = 4$). For $0 \leqslant Q \leqslant 4$, the Q-state Potts model has a critical point at which the clusters percolate and have a conformal invariant measure. Natural observables are the cluster connectivities, given by the probability that a number of lattice points belong to the same or different clusters [9–11]. The conjecture of Delfino and Viti on the three-point connectivities [12] has been at the origin of a series of papers [13–20] which unveiled important insights on the still unknown bootstrap solution.

In this paper we focus on the *two-point* connectivity *on a torus*. This study is motivated by two facts:

- In order to increase the number of samplings, Monte Carlo measurements are conveniently taken on doubly periodic lattices [19]: a precise knowledge of topological corrections is therefore needed to extract the scaling plane limit which is then compared to the CFT on the sphere predictions.
- The torus topological effects encode informations on the set of states and on the three-point functions, which are the basic ingredients to solve a CFT.

In section 2 we review notions of CFT on a torus and provide the general formulas we will need. In section 3 we define the lattice observables and we provide analytical results on their universal finite size behaviours. These results are then compared with the numerical results in section 5, where details of the simulations are also discussed. The final conclusions are found in section 6.

2. Conformal field theory on a torus

2.1. Virasoro algebra and its representation

Consider first a CFT on a plane $z \in (\mathbb{C} \bigcup \{\infty\})$ [21] with $T(z)$ and $\bar{T}(\bar{z})$ the holomorphic and anti-holomorphic component of the stress energy-tensor. The holomorphic stress-energy modes $L_n^{(z)}$, defined in (A.1) form the Virasoro algebra $\mathcal{V}_c$ with central charge c:

$$\left[L_n^{(z)}, L_m^{(z)}\right] = (n-m)L_{n+m}^{(z)} + \frac{c}{12} n(n^2-1)\delta_{n,m}. \tag{2.1}$$

The anti-holomorphic modes $\bar{L}_n^{(z)}$ are analogously defined and form a second Virasoro algebra $\overline{\mathcal{V}}_c$, with the same central charge, that commutes with (2.1).

A highest-weight representation of $\mathcal{V}_c$ is labelled by the conformal dimension Δ: it contains the primary field V_Δ, $L_n|V_\Delta\rangle = 0$ for $n > 0$, and its descendants, obtained by acting with the negative modes on the primary state. Given a Young diagram $Y = \{n_1, n_2 \cdots\}$, with $n_i \in \mathbb{N}, n_i \leqslant n_{i+1}$, the fields

$$V_\Delta^{(Y)} = L_{-Y}^{(z)} V_\Delta = L_{-n_1}^{(z)} L_{-n_2}^{(z)} \cdots V_\Delta \quad (V_\Delta^{(\{0\})} = V_\Delta) \tag{2.2}$$

J. Stat. Mech. (2020) 023101

form a complete basis of the Δ representation. The descendant $V_\Delta^{(Y)}$ has total dimension $\Delta + |Y|$, where $|Y| = \sum n_i$ is called the level of the descendant. For general Δ, the number of independent descendants is therefore the number of partitions of $|Y|$. The inner product $H_\Delta(Y, Y')$ between descendants is defined as:

$$H_\Delta(Y, Y') = \lim_{z\to\infty} z^{2\Delta} \left\langle V_\Delta(z) L_Y^{(0)} L_{-Y'}^{(0)} V_\Delta(0) \right\rangle, \tag{2.3}$$

and is completely defined by the algebra (2.1). For certain values of Δ, see (2.9), the representations are degenerate: they contain a descendant field, usually called the null state, which has vanishing norm. For unitary CFTs, the null state is set to zero. Otherwise, one can have CFTs where null states are not vanishing, like for instance in [22]. For the sake of simplicity, we will continue to denote the descendant states as $V_\Delta^{(Y)}$ even when the presence of a vanishing null state makes their number smaller than the number of partitions. In this case, the notation Y is meant to label the independent non-vanishing descendants.

The spectrum $\mathcal{S}$ of a CFT is formed by the representations of $\mathcal{V}_c \otimes \overline{\mathcal{V}}_c$ appearing in the theory and labelled by the holomorphic and anti-holomorphic dimensions $\Delta, \bar{\Delta}$. In order to simplify the formulas, we use the notations $(\Delta)_i = \Delta_i, \bar{\Delta}_i$ and $(\Delta, Y)_i = (\Delta_i, Y_i), (\bar{\Delta}_i, \bar{Y}_i)$. In these notations, a $\mathcal{V}_c \otimes \overline{\mathcal{V}}_c$ primary field and its descendants are

$$V_{(\Delta)}(z, \bar{z}) = V_\Delta(z) V_{\bar{\Delta}}(\bar{z}), \quad V_{(\Delta,Y)}(z, \bar{z}) = L_{-Y}^{(z)} \bar{L}_{-\bar{Y}}^{(\bar{z})} V_\Delta(z) V_{\bar{\Delta}}(\bar{z}). \tag{2.4}$$

The product of two primary fields (OPE) can be expanded in terms of the states appearing in the spectrum $\mathcal{S}$ [21]:

$$V_{(\Delta)_1}(z, \bar{z})\, V_{(\Delta)_2}(0) \to a_{(\Delta)_1,(\Delta)_2}^{(\Delta,Y)_3}(z, \bar{z})\, V_{(\Delta,Y)_3}(0), \tag{2.5}$$

where the coefficients are factorised as:

$$a_{(\Delta)_1,(\Delta)_2}^{(\Delta,Y)_3}(z, \bar{z}) = C_{(\Delta)_1,(\Delta)_2}^{(\Delta)_3}\, \beta_{\Delta_1,\Delta_2}^{(\Delta_3,Y_3)}(z)\, \beta_{\bar{\Delta}_1,\bar{\Delta}_2}^{(\bar{\Delta},\bar{Y}_3)}(\bar{z}). \tag{2.6}$$

One factor is the (model dependent) structure constant $C_{(\Delta)_1,(\Delta)_2}^{(\Delta)_3}$, the other factor is fixed by the algebra (2.1):

$$\beta_{\Delta_1,\Delta_2}^{(\Delta_3,Y_3)}(z) = z^{-\Delta_1-\Delta_2+\Delta_3+|Y|} \sum_{\substack{Y' \\ |Y'|=|Y|}} H_{\Delta_3}^{-1}(Y, Y')\, \Gamma_{(\Delta_2,\{0\}),(\Delta_1,\{0\}))}^{(\Delta_3,Y')}, \tag{2.7}$$

where:

$$\Gamma_{(\Delta_1,Y_1),(\Delta_2,Y_3)}^{(\Delta_3,Y_3)} = \frac{\left\langle L_{-Y_3}^{(\infty)}\, V_{\Delta_3}(\infty) L_{-Y_2}^{(1)} V_{\Delta_2}(1) L_{-Y_1}^{(0)} V_{\Delta_1}(0) \right\rangle}{\langle V_{\Delta_3}(\infty) V_{\Delta_2}(1) V_{\Delta_1}(0) \rangle}. \tag{2.8}$$

Under the replacement $\Delta_i \to \bar{\Delta}_i$, the above formulas define $\beta_{\bar{\Delta}_1,\bar{\Delta}_2}^{(\Delta_3,\bar{Y}_3)}(\bar{z})$ too. The three-point function (2.8) can be computed in an efficient way by the recursion formulas in [23].

In the study of the critical random Potts model, the following series of notations turns out to be very convenient. The conformal dimension can be parametrised as follows

J. Stat. Mech. (2020) 023101

$$\Delta = \Delta_{(r,s)} = \frac{c-1}{24} + \frac{1}{4}\left(r\beta - \frac{s}{\beta}\right)^2. \tag{2.9}$$

A representation is degenerate if $r, s \in \mathbb{N}^*$, and has a null state at level rs. The symbols

$$V_{\Delta_{(r,s)},\Delta_{(r,s)}} = V_{(r,s)^D}, \quad V_{\Delta_{(r,s)},\Delta_{(r,-s)}} = V_{(r,s)} \tag{2.10}$$

indicate the diagonal and non-diagonal primary fields and the notations

$$(r,s)^D, \quad (r,s) \tag{2.11}$$

denote the representations associated to $V_{(r,s)^D}$ and $V_{(r,s)}$ respectively. This allows us to use a lighter notations for the structure constants, for instance:

$$C^{(r,s)^D}_{(r_1,s_1),(r_2,s_2)} = C^{(\Delta_{r_3,s_3},\Delta_{r_3,s_3})}_{(\Delta_{r_1,s_1},\Delta_{r_1,-s_1}),(\Delta_{r_2,s_2},\Delta_{r_2,-s_2})}. \tag{2.12}$$

A set of these representations is denoted as

$$\mathcal{S}^D_X = \{(r,s)^D\}_{(r,s)\in X}, \quad \mathcal{S}_X = \{(r,s)\}_{(r,s)\in X}, \tag{2.13}$$

where X is a given set of pairs (r,s). A third set type is $\mathcal{S}^{\text{quot}}_X$ that contains the degenerate representations with vanishing null state.

2.2. Torus correlation functions

So far we have reviewed the properties of a CFT that do not depend on the topology of the surface. The theory of Virasoro algebra on general Riemann surfaces can be found in [24]. Let us consider now a CFT on a torus with periods ω_1 and ω_2. In the numerical simulations one usually considers doubly periodic rectangular lattices of size $M \times N$, where $M, N \in \mathbb{R}_{>0}$. We therefore set:

$$\omega_1 = \mathrm{i}M, \quad \omega_2 = N, \quad \tau = \frac{\omega_1}{\omega_2} = \mathrm{i}\frac{M}{N}, \quad q = \mathrm{e}^{2\pi\mathrm{i}\tau}. \tag{2.14}$$

The results we will obtain can be of course generalized to the case $\mathrm{Re}\,\tau \neq 0$. In the following, we represent the torus as a finite cylinder of size N with the ends, at distance $M = O(N)$, glued together. Accordingly, we use the map

$$w = -\mathrm{i}\,\frac{N}{2\pi}\ln z \tag{2.15}$$

sending the plane (z) to an infinite cylinder (w) of size N.

We define a general field $V^{\mathcal{C},N}_{(\Delta,Y)}$ on the cylinder of size N as:

$$V^{\mathcal{C},N}_{(\Delta,Y)}(w,\bar{w}) = L^{\mathcal{C},(w)}_{-Y}\bar{L}^{\mathcal{C},(\bar{w})}_{-\bar{Y}}\, V^{\mathcal{C},N}_{(\Delta)}(w,\bar{w}), \tag{2.16}$$

where $L^{\mathcal{C},(w)}_{-n}$, $\bar{L}^{\mathcal{C},(w)}_{-n}$ are the conformal generators on the cylinder. They are related to the fields on the cylinder of size $N = 1$ by a factor arising from their transformation under (2.15), see appendix :

$$V^{\mathcal{C},N}_{(\Delta,Y)}(w,\bar{w}) = \left(\frac{2\pi}{N}\right)^{\Delta+\bar{\Delta}+|Y|+|\bar{Y}|} V^{\mathcal{C},N=1}_{(\Delta,Y)}(w,\bar{w}). \tag{2.17}$$

Henceforth, we will often omit the symbol $\mathcal{C}, N$ when the field on the cylinder is a primary, i.e. $V^{\mathcal{C},N}_{(\Delta)}(w) \to V_{(\Delta)}(w)$. The relation between $L^{\mathcal{C},(w)}_{-n}$ and $L^{(z)}_{-n}$ is obtained using the transformation of T under the map (2.15) see appendix .

The torus function $\left\langle \prod_i V_{(\Delta_i)} \right\rangle_\tau$ corresponds to the trace of the ons. The one-point torus correlation function can be associated with the following diagram:

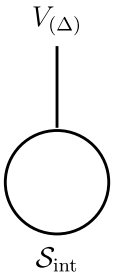

where $\mathcal{S}_{\rm int} \in \mathcal{S}$ is the set of representations that propagate along the M direction and whose fusion with themselves contains the representation (Δ). It takes the form:

$$\langle V_{(\Delta)} \rangle_\tau = \frac{1}{Z} \mathrm{Tr}_{\mathcal{S}_{\rm int}} \left(q^{L_0^{\mathcal{C},(\infty)}} \bar{q}^{\bar{L}_0^{\mathcal{C},(\infty)}} V_{(\Delta)}(0) \right) = \frac{1}{Z} \sum_{(\Delta_{\rm int}) \in \mathcal{S}_{\rm int}} C^{(\Delta)}_{(\Delta_{\rm int}),(\Delta_{\rm int})} \mathcal{F}^{\Delta_{\rm int}}_{\Delta}(q)\, \mathcal{F}^{\bar{\Delta}_{\rm int}}_{\bar{\Delta}}(\bar{q}), \tag{2.18}$$

where $L_0^{\mathcal{C},(\infty)} = L_0^{(0)} - \frac{c}{24}$ and $\mathcal{F}^{\Delta_{\rm int}}_{\Delta}(q)$ is the torus conformal block:

$$\begin{aligned} \mathcal{F}^{\Delta_{\rm int}}_{\Delta}(q) &= q^{\Delta_{\rm int} - \frac{c}{24}}\, \bar{q}^{\bar{\Delta}_{\rm int} - \frac{c}{24}} \sum_{\substack{Y,Y' \\ |Y|=|Y'|}} q^{|Y|} H^{-1}_{\Delta_{\rm int}}(Y,Y')\ \Gamma^{(\Delta_{\rm int},Y')}_{(\Delta_{\rm int},Y),(\Delta,\{\emptyset\})} \\ &= q^{\Delta_{\rm int} - \frac{c}{24}}\, \bar{q}^{\bar{\Delta}_{\rm int} - \frac{c}{24}} \left(1 + \frac{2\Delta_{\rm int} + \Delta(\Delta-1)}{2\Delta_{\rm int}} q + \cdots \right) \end{aligned} \tag{2.19}$$

see (2.3)–(2.8). The torus partition function Z can be related to the identity one-point function, for which $\mathcal{S}_{\rm int} = \mathcal{S}$,

$$Z = \mathrm{Tr}_{\mathcal{S}} \left(q^{L_0^{\mathcal{C},(\infty)}} \bar{q}^{\bar{L}_0^{\mathcal{C},(\infty)}} \right) = \sum_{(\Delta_{\rm int}) \in \mathcal{S}} \mathcal{F}^{\Delta_{\rm int}}_{0}(q)\, \mathcal{F}^{\bar{\Delta}_{\rm int}}_{0}(\bar{q}). \tag{2.20}$$

The computation of $\mathcal{F}^{\Delta_{\rm int}}_{0}(q)$ using recursion relations is discussed in [25].

The s-channel expansion of the torus two-point function $\left\langle V_{(\Delta)_1}(w) V_{(\Delta)_2}(0) \right\rangle_\tau$ is described by the diagram:

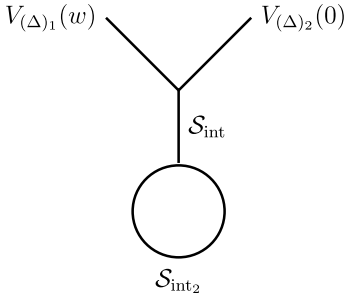

https://doi.org/10.1088/1742-5468/ab6331

J. Stat. Mech. (2020) 023101

where $\mathcal{S}_{\rm int}$ contains the fields appearing in the fusion $V_{(\Delta)_1}V_{(\Delta)_2}$ and $\mathcal{S}_{{\rm int}_2}$ is the spectrum of the one-point torus function of the fields in $\mathcal{S}_{\rm int}$. One can show, see appendix, that the two-point torus function can be expanded as:

$$\langle V_{(\Delta)_1}(w)V_{(\Delta)_2}(0)\rangle_\tau = \left(\frac{N}{2\pi}\right)^{-\Delta_1-\Delta_2-\bar\Delta_1-\bar\Delta_2} \sum_{(\Delta,Y)_{\rm int}\in\mathcal{S}_{\rm int}} a^{(\Delta,Y)_{\rm int}}_{(\Delta)_1,(\Delta)_2}\left(\frac{2\pi w}{N}\right)\left\langle V^{\mathcal{C}}_{(\Delta,Y)}\right\rangle_\tau . \tag{2.21}$$

3. Q-Potts random cluster model

Let us consider a rectangular lattice $N\times M$ with periodic boundary conditions in the two directions. The edges of the graph carry a bond with probability p, or no bond with probability $1-p$. According to these bonds, the lattice is split into a disjoint union of connected clusters. The random cluster Q-state Potts model [26] is defined by the partition function

$$\mathcal{Z}_Q = \sum_{\mathcal{G}} Q^{\#\,\text{clusters}}p^{\#\,\text{bonds}}(1-p)^{\#\,\text{edges without bond}}. \tag{3.1}$$

At the critical value

$$p = p_c = \frac{\sqrt{Q}}{\sqrt{Q}+1}, \tag{3.2}$$

the probability that there exists a percolating cluster jumps from 0 to 1, in the limit of infinite lattice size. The model becomes conformally invariant in the scaling limit, and has central charge c:

$$c = 1-6\left(\beta-\beta^{-1}\right)^2, \qquad Q = 4\cos^2\pi\beta^2 \quad \text{with} \quad \frac{1}{2}\leqslant\beta^2\leqslant 1\ . \tag{3.3}$$

The scaling limit Z_Q of the Potts partition function (3.1) at the critical point (3.2) was computed in [27]:

$$Z_Q = \text{equation (4.8) of [27]}, \quad \text{with } e_0\to 2-2\beta^2, \quad g\to 4\beta^2, \quad h_{s,r}\to\Delta_{(-2r,\frac{s}{2})}. \tag{3.4}$$

The corresponding total spectrum is:

$$\mathcal{S}^{\rm Potts} = \mathcal{S}^{D,\rm quot}_{(1,\mathbb{N}^*)} \bigcup_{\substack{j\geqslant 2\\ M|j,p\wedge M=1}} \mathcal{S}_{(j,\mathbb{Z}+\frac{p}{M})} \bigcup \mathcal{S}_{(0,\mathbb{Z}+\frac{1}{2})}. \tag{3.5}$$

The multiplicities associated to the above sectors have also been computed [27] and, for general Q, assume general real values. We refer the reader to [18] for a derivation of (3.5) from the representations of Temperley–Lieb type algebras. $\mathcal{S}^{D,\rm quot}_{(1,\mathbb{N}^*)}$ is the thermal sector [28] and contains the identity and the energy field:

$$\text{Identity field} = V_{(1,1)^D}, \quad \text{Energy field} = V_{(1,2)^D}.$$

The space of n-point cluster connectivities has been defined in [9]. Here we will focus only on the two-point connectivities:

J. Stat. Mech. (2020) 023101

$$p_{12} = \text{Probability}(w_1, w_2 \text{ are in the same cluster}). \tag{3.6}$$

At the critical point (3.2) and in the plane limit $N, M \to \infty$, the Coulomb gas approach [29] determines the scaling limit of the probability p_{12} :

$$\text{Plane scaling limit : } \; p_{12} = c_0 \, |w|^{-4\Delta_{(0,\frac{1}{2})}}, \quad w = w_1 - w_2, \tag{3.7}$$

where c_0 is a non-universal constant, see section 5. From the above equation one sees that, in the plane, the two-point connectivity is related to the plane two-point function of the

$$\text{Connectivity field} = V_{(0,\frac{1}{2})}, \tag{3.8}$$

belonging to the magnetic sector $\mathcal{S}_{(0,\mathbb{Z}+\frac{1}{2})}$ [30]. It is natural to assume that the relation between p_{12} and the $V_{(0,\frac{1}{2})}$ two-point function holds on the torus, i.e.:

$$\text{Torus scaling limit : } p_{12} = c_0 \, \left\langle V_{(0,\frac{1}{2})}(w) V_{(0,\frac{1}{2})}(0) \right\rangle_\tau, \quad w = w_1 - w_2. \tag{3.9}$$

Let us mention that a rigorous proof of (3.2) has been obtained recently in [31] where the behaviour of the probability (3.6) in the sub-critical regime $p < p_c$ and on the torus was also studied.

4. Two-point Potts torus connectivity

According to Monte Carlo simulations (see section 5) while $(0, \frac{1}{2})$ is the field in (3.5) with the smallest non-zero conformal dimension, the leading topological correction is given by the energy state $(1,2)^D$. The contribution from the second thermal operator $(1,3)^D$ is also visible at $Q \sim 3$. Based on these observations, we assume that $\left\langle V_{(0,\frac{1}{2})}(w) V_{(0,\frac{1}{2})}(0) \right\rangle_\tau$ is given by (2.21) with $\mathcal{S}_{\text{int}} = \mathcal{S}^{D,\text{quot}}_{(1,\mathbb{N}^*)}$. In particular we compute the contributions of the first three dominant channels:

$$\mathcal{S}_{\text{int}} = \{(1,1)^D, (1,2)^D, (1,3)^D\}. \tag{4.1}$$

The agreement between Monte Carlo and analytic results presented below confirms that this truncated spectrum (4.1) provides a good approximation to $\left\langle V_{(0,\frac{1}{2})}(w) V_{(0,\frac{1}{2})}(0) \right\rangle_\tau$. Some arguments going in this direction come also from the analysis in [18, 20] where the spectrum of all independent four-point connectivities has been determined. In particular, it was shown that the asymptotic of the probability $p_{12} \cap p_{34}$ (related to $P_0 + P_1$ in [20]), in the limit $z_2 - z_1 \to 0$ and $z_3 - z_2 \gg 1$, is dominated by the low lying states $(1,1)^D, (1,2)^D, (1,3)^D, (2,0), \cdots$. In this limit one expects that $p_{12} \cap p_{34} \sim \; p_{12} \, p_{34} +$ corrections, where the corrections are produced by the configurations which correlate the p_{12} and p_{13} probabilities and which are associated to the state $(2,0)$ [20].

J. Stat. Mech. (2020) 023101

Table 1. c_0 and c_1 from a fit of the numerical data to the form (5.1). The last column contains the analytical determination in (4.11*a*).

Q	c_0	c_1	$c_{(1,2)}$
1	0.747 19	0.356	0.357 07
1.25	0.733 23	0.392	0.393 023
$2+\cos\frac{3\pi}{5}$	0.726 93	0.414	0.411 442
1.5	0.721 78	0.4343	0.427 244
1.75	0.711 99	0.459	0.458 989
2.0	0.703 37	0.488	0.488 863
2.25	0.695 56	0.518	0.517 293
2.5	0.688 27	0.551	0.544 607
2.75	0.681 13	0.578	0.571 079
3.0	0.673 76 (2)	0.599	0.596 962
3.25	0.665 55 (5)	0.627	0.622 532
$2+\sqrt{2}$	0.659 02 (7)	0.642	0.639 326

In the limit:

$$N \to \infty, \quad \frac{M}{N} \to O(1), \quad 1 \ll w \ll N, \tag{4.2}$$

using the expression for the two-point function (2.21) with the internal spectrum (4.1) we obtain the following N^{-1} expansion

$$\begin{aligned}\left\langle V_{(0,\frac{1}{2})}(w)V_{(0,\frac{1}{2})}(0)\right\rangle_\tau &= |w|^{-4\Delta_{(0,\frac{1}{2})}} \sum_{X\in\{(1,1)^D,(1,2)^D,(1,3)^D\}} C^X_{(0,\frac{1}{2}),(0,\frac{1}{2})} \left|\frac{2\pi w}{N}\right|^{2\Delta_X} (\langle V_X\rangle_\tau \\ &+ \left(\frac{2\pi}{N}\right)^2 \beta_X^{\{2\}} \left(w^2 \left\langle L^{\mathcal{C},(0)}_{-2} V_X\right\rangle_\tau + \bar{w}^2 \left\langle \bar{L}^{\mathcal{C},(0)}_{-2} V_X\right\rangle_\tau\right) \\ &+ \left(\frac{2\pi}{N}\right)^3 \beta_X^{\{3\}} \left(w^3 \left\langle L^{\mathcal{C},(0)}_{-3} V_X\right\rangle_\tau + \bar{w}^3 \left\langle \bar{L}^{\mathcal{C},(0)}_{-3} V_X\right\rangle_\tau\right) + \cdots\Bigg),\end{aligned} \tag{4.3}$$

where we set $\beta_X^Y = \beta^{(\Delta_X,Y)}_{\Delta_{(0,\frac{1}{2})},\Delta_{(0,\frac{1}{2})}}$. Note that descendants of the type $L^{\mathcal{C}}_{-1}L^{\mathcal{C}}_{-Y}V_X$ are total derivatives and their torus one-point functions vanish.

The main message here is that the leading topological correction for the two-point connectivity is given, for $1 \leqslant Q \leqslant 4$ by the energy $(1,2)^D$ state. Given two-points w_1, w_2 on a torus (2.14) and at distance $r = |w_1 - w_2|$, the scaling limit of the probability (3.6) is:

$$\begin{aligned}p_{12} = \frac{c_0}{r^{4\Delta_{(0,\frac{1}{2})}}}\Bigg[1 + \left(\frac{r}{N}\right)^{2\Delta_{(1,2)}} \left(\frac{(2\pi)^{2\Delta_{(1,2)}}}{Z_Q(q)}(Q-1)\left[C^{(1,2)^D}_{(0,\frac{1}{2}),(0,\frac{1}{2})}\right]^2 q^{2\left(\Delta_{(0,\frac{1}{2})}-\frac{c}{24}\right)}(1+O(q))\right) \\ + O\left(\left(\frac{r}{N}\right)^2\right)\Bigg]\end{aligned} \tag{4.4}$$

where c_0 is a non-universal constant evaluated in table 1, and $C^{(1,2)^D}_{(0,1/2),(0,1/2)}$ is given in (4.16). At the critical percolation $Q = 1$ point, we have:

J. Stat. Mech. (2020) 023101

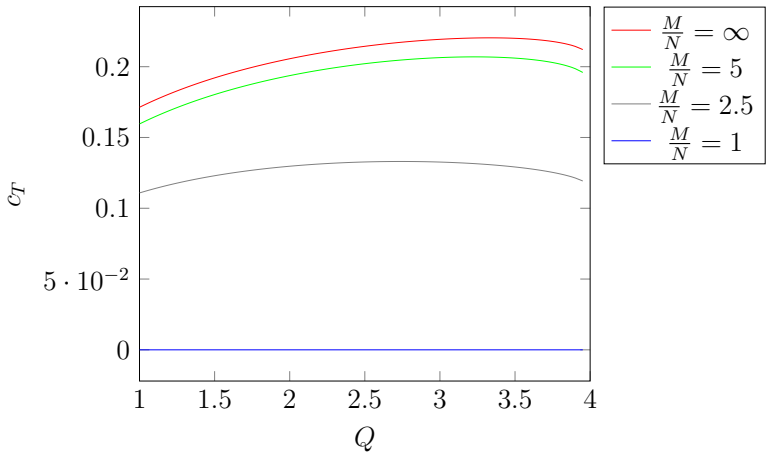

Figure 1. The contribution c_T of the stress-energy tensor, as a function of Q and for different values of the aspect ratio $\frac{M}{N}$.

$$p_{12} = \frac{c_0}{r^{\frac{5}{24}}}\left[1 + \left(\frac{r}{N}\right)^{\frac{5}{4}}\left((2\pi)^{\frac{5}{4}}\pi\sqrt{3}\left(\frac{4}{9}\frac{\Gamma(\frac{7}{4})}{\Gamma(\frac{1}{4})}\right)^2 e^{-\frac{5\pi}{24}\frac{M}{N}} + O\left(e^{-\frac{53}{24}\pi\frac{M}{N}}\right)\right) + O\left(\left(\frac{r}{N}\right)^2\right)\right]. \tag{4.5}$$

The formula (4.4) represents, at the best of our knowledge, a new analytic result on the universal properties of general Q random Potts critical clusters and, in particular, of the critical percolation clusters (4.5). The derivation of (4.4) and (4.5), of the next $\frac{r}{N}$ sub-leading topological terms and of the systematic computation of the q expansion, are given below.

4.1. Identity channel contributions

The leading contribution to (4.3) comes from the identity. In particular we have:

$$\text{Leading} \ : \ |w|^{-4\Delta_{(0,\frac{1}{2})}} \quad (\text{plane limit}), \tag{4.6a}$$

$$\text{Sub-leading} \ : \ |w|^{-4\Delta_{(0,\frac{1}{2})}}\left[\left(\frac{w}{N}\right)^2 c_T + \left(\frac{\bar{w}}{N}\right)^2 c_{\bar{T}}\right] \tag{4.6b}$$

$$\text{Next to sub-leading} : O\left(\frac{1}{N^4}\right). \tag{4.6c}$$

The dominant term corresponds to the plane limit while the sub-leading factors c_T and $c_{\bar{T}}$:

$$c_T = \frac{2\Delta_{(0,\frac{1}{2})}}{c}\left\langle T^{\mathcal{C}}\right\rangle_\tau, \quad c_{\bar{T}} = \frac{2\Delta_{(0,\frac{1}{2})}}{c}\left\langle \bar{T}^{\mathcal{C}}\right\rangle_\tau \tag{4.7}$$

are proportional to the stress energy one-point function, with

$$\langle T^{\mathcal{C}}\rangle_\tau = \mathrm{i}\pi\partial_\tau \log Z_Q. \tag{4.8}$$

J. Stat. Mech. (2020) 023101

In figure 1 we plot c_T as a function of Q and for different τ, i.e. for different ratios $\frac{M}{N}$: for a square torus, $M=N$ and $\langle T^{\mathcal{C}}\rangle_\tau = \langle \bar{T}^{\mathcal{C}}\rangle_\tau = 0$, for all Q. This is the reason the N^{-2} corrections were not visible in the fits in [20]. In the cylinder limit $M/N \to \infty$ one recovers the well known result $\langle T^{\mathcal{C}}\rangle_{i\infty} = (2\pi)^2 \frac{c}{24}$. It is interesting to stress that the $\lim_{c\to 0} \frac{2\Delta_{(0,\frac{1}{2})}}{c} \left\langle T^{\mathcal{C}}\right\rangle_\tau$ is finite and different from zero. No subtleties, arising from the existence at $c=0$ of a logarithmic partner of the stress energy tensor, seem to emerge. Indeed one can write

$$Z = 1 + O(Q-1) \tag{4.9}$$

which gives a finite limit for

$$c_T = -\frac{2\Delta_{(0,\frac{1}{2})}}{c} 2\pi^2 q\partial q Z. \tag{4.10}$$

The next corrections from the identity channel appear at order N^{-4} and are related to the propagation of the identity descendants $\langle T^{\mathcal{C}}\bar{T}^{\mathcal{C}}\rangle_\tau$, $\langle L^{\mathcal{C}}_{-4}\mathrm{Id}\rangle_\tau$ and $\langle \bar{L}^{\mathcal{C}}_{-4}\mathrm{Id}\rangle_\tau$.

4.2. Energy channel contributions

Besides the identity, the energy $V_{(1,2)^D}$ field has the lowest dimension in $\mathcal{S}^{D,\mathrm{quot}}_{(1,\mathbb{N}^*)}$. The $(1,\,2)^D$ contribution to (4.3) is given by

$$\text{Leading}: |w|^{-4\Delta_{(0,\frac{1}{2})}} \left(\frac{|w|}{N}\right)^{2\Delta_{(1,2)}} c_{(1,2)}, \tag{4.11a}$$

$$\text{Sub-leading}: O\left(\frac{1}{N^{2\Delta_{(1,2)}+4}}\right) \tag{4.11b}$$

where:

$$c_{(1,2)} = (2\pi)^{2\Delta_{(1,2)}}\ C^{(1,2)^D}_{(0,\frac{1}{2}),(0,\frac{1}{2})} \left\langle V_{(1,2)^D}\right\rangle_\tau . \tag{4.12}$$

We can compute the one-point function $\left\langle V_{(1,2)^D}\right\rangle_\tau$ by using the vanishing of the $(1,2)^D$ null state, which determines the OPE [21]:

$$V_{(1,2)} \times V_{(r,s)} \to V_{(r,s+1)} \oplus V_{(r,s-1)} \tag{4.13}$$

$(0,\frac{1}{2})$ is the only representation which satisfies both the above OPE and

$$V_{(1,2)} \times V_{(0,\frac{1}{2})} \to V_{(0,\frac{1}{2})}. \tag{4.14}$$

Therefore the one-point function $\left\langle V_{(1,2)^D}\right\rangle_\tau$ gets contribution only from the propagation of the $(0,\frac{1}{2})$ state, i.e. $\mathcal{S}_{\mathrm{int}} = \{(0,\frac{1}{2})\}$ in (2.18). This property was pointed out in [32] where the energy one-point function for minimal models was computed in terms of a Coulomb gas integral. Collecting all these facts, we obtain:

J. Stat. Mech. (2020) 023101

$$\langle V_{(1,2)^D}\rangle_\tau = \frac{Q-1}{Z_Q}\, C^{(1,2)^D}_{(0,\frac{1}{2}),(0,\frac{1}{2})} \left|\mathcal{F}^{\Delta_{(0,\frac{1}{2})}}_{\Delta_{(1,2)}}(q)\right|^2$$
$$= \frac{Q-1}{Z_Q}\, C^{(1,2)^D}_{(0,\frac{1}{2}),(0,\frac{1}{2})}\, |q|^{2\left(\Delta_{(0,\frac{1}{2})}-\frac{c}{24}\right)} \left|1+\frac{2\Delta_{(0,\frac{1}{2})}+\Delta_{(1,2)}(\Delta_{(1,2)}-1)}{2\Delta_{(0,\frac{1}{2})}}q+\cdots\right|^2 \tag{4.15}$$

where the factor $Q-1$ comes from the multiplicity of the $\mathcal{S}_{(0,\mathbb{Z}+\frac{1}{2})}$ sector computed in [27] and the structure constant is given by:

$$C^{(1,2)^D}_{(0,\frac{1}{2}),(0,\frac{1}{2})} = \beta^4 \frac{\gamma\left(-\frac{1}{2}\right)}{\gamma\left(-\frac{1}{2\beta^2}\right)}\sqrt{\gamma\left(\frac{1}{\beta^2}\right)\gamma\left(2-\frac{2}{\beta^2}\right)}, \quad \gamma(x)=\frac{\Gamma(x)}{\Gamma(1-x)}. \tag{4.16}$$

The next energy contributions come from the descendants $L^{\mathcal{C}}_{-2}V_{(1,2)^D}$ and $\bar{L}^{\mathcal{C}}_{-2}V_{(1,2)^D}$. The null state in the representation $(1,2)^D$ is

$$\chi = \left(-\beta^2(L^{(1)}_{-1})^2 + L^{(1)}_{-2}\right) V_{(1,2)^D}(1). \tag{4.17}$$

Using (A.4)

$$L^{\mathcal{C},(0)}_{-2} = \left(\frac{2\pi \mathrm{i}}{N}\right)^2 \left(L^{(1)}_{-2} - \frac{c}{24} - \frac{13}{12}L^{(1)}_0\right) \tag{4.18}$$

and setting the null vector to zero

$$L^{(1)}_{-2}V_{(1,2)^D}(1) = \beta^2 (L^{(1)}_{-1})^2\, V_{(1,2)^D}(1) \tag{4.19}$$

leads to

$$\left\langle L^{\mathcal{C},(0)}_{-2}V_{(1,2)^D}(0)\right\rangle_\tau = \left\langle \bar{L}^{\mathcal{C},(0)}_{-2}V_{(1,2)^D}(0)\right\rangle_\tau = 0, \tag{4.20}$$

which explains why the sub-leading corrections in (4.11*a*) are found in the fourth level descendants of the energy (the third level descendant is a total derivative). Using the expression of the one-point function (4.15) in (4.11*a*) with $r=|w|$, one obtains our result (4.4).

At the critical percolation point $Q=1$, the bond probabilities, associated to the energy field (see next section), are independent. The CFT energy one-point function (4.15), which actually probes the fluctuation induced corrections to the bulk constant value, vanishes at $Q=1$. On the other hand, the vanishing of the one-point function is exactly cancelled by the divergence in the structure constant (4.16), thus providing a non-zero contribution to $\lim_{Q\to 1} C^{(1,2)^D}_{(0,1/2),(0,1/2)}\langle V_{(1,2)^D}\rangle_\tau$. The result is given in (4.5).

When $M\neq N$, we have seen that we have a N^{-2} contribution of the energy tensor to the topological corrections. Even if this term is sub-leading in the parameter $\frac{r}{N}$, $r=|w|$, in finite size simulations it can interfere or even be dominant with respect to the energy contribution. In figure 2 we plot as function of Q, and for different ratios $\frac{M}{N}$, the regimes of $\frac{r}{N}$ dominated by the energy (below the curve) or by the stress-energy (above the curve) topological corrections:

J. Stat. Mech. (2020) 023101

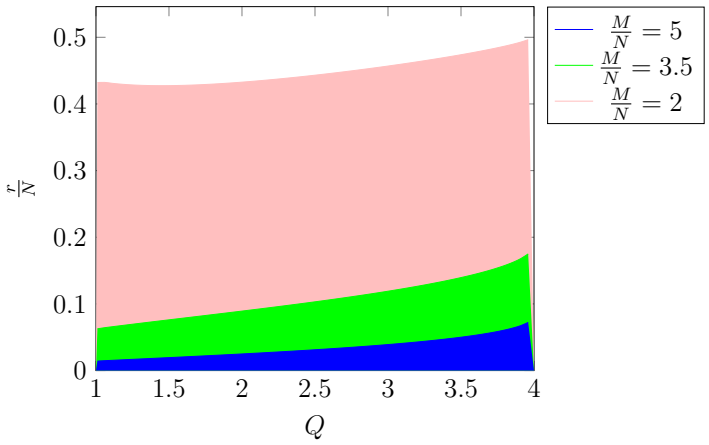

Figure 2. Regimes of $\frac{r}{N}$ dominated by the energy (resp. the stress-energy tensor) contribution below (resp. above) the curve, as a function of Q, and for different ratios $\frac{M}{N}$.

4.3. $(1, 3)^D$ channel contributions

$(1,3)^D$ has a dimension $4 \geqslant 2\Delta_{(1,3)} \geqslant 2$ for $1 \leqslant Q \leqslant 4$, decreasing with Q. Despite this relatively high dimension, the term

$$\text{Leading} : |w|^{-4\Delta_{(0,\frac{1}{2})}} \left(\frac{|w|}{N}\right)^{2\Delta_{(1,3)}} c_{(1,3)} \tag{4.21a}$$

$$\text{Sub-leading} : O\left(\frac{1}{N^{2\Delta_{(1,3)}+2}}\right) \tag{4.21b}$$

where:

$$c_{(1,3)} = (2\pi)^{2\Delta_{(1,3)}} \; C^{(1,3)^D}_{(0,\frac{1}{2}),(0,\frac{1}{2})} \left\langle V_{(1,3)^D}(0)\right\rangle_\tau \tag{4.22}$$

provides a visible contribution when $Q \geqslant 3$, see next section 5.4.

We consider then $\left\langle V_{(1,3)^D}\right\rangle_\tau$. Differently from the case of the energy field, the fusion rule imposed by the vanishing of the $(1,3)^D$ null state:

$$V_{\Delta_{(1,3)}} \times V_{\Delta_{(r,s)}} \to V_{\Delta_{(r,s+2)}} \oplus V_{\Delta_{(r,s)}} \oplus V_{\Delta_{(r,s-2)}}, \tag{4.23}$$

does not fix the representations contributing to its one-point function, since the fusion $V_{\Delta_{(1,3)}} \times V_{\Delta_{(r,s)}} \to V_{\Delta_{(r,s)}}$ is allowed for all r, s. This can be seen also from the fact that the structure constant $C^{(1,3)^D}_{(\Delta),(\Delta)}$ is different from zero for any Δ and c [21]. Parametrising Δ as in (2.9), one has, for three diagonal (spinless) fields [33]:

$$C^{(1,3)^D}_{(r,s)^D,(r,s)^D} = \sqrt{\frac{\gamma^3(\frac{1}{\beta^2})\gamma(2-\frac{2}{\beta^2})\gamma(2-\frac{3}{\beta^2})}{\gamma(\frac{2}{\beta^2})} \frac{\gamma^2(r+\frac{1-s}{\beta^2})}{\gamma^2(1+r-\frac{1+s}{\beta^2})}}. \tag{4.24}$$

The above value of the structure constant can be derived either from the vanishing of the third level null state of $(1,3)^D$ or from a Coulomb gas integral, as the three vertex fields satisfy the charge neutrality condition. One can expect on solid grounds

J. Stat. Mech. (2020) 023101

that $C^{(1,3)^D}_{(r,s)^D,(r,s)^D}$ describes certain three-point correlation functions in the Q-state Potts model. In [15] for instance, the structure constant $C^{(1,3)^D}_{(1,0),(1,0)}$ has been checked to correspond to the scaling limit of certain lattice transfer matrix amplitudes. In the case of two non-diagonal fields, $C^{(1,3)^D}_{(r,s),(r,s)}$ has been shown in [15, 34] to be given by $C^{(1,3)^D}_{(r,s),(r,s)} = \sqrt{C^{(1,3)^D}_{(r,s)^D,(r,s)^D} C^{(1,3)^D}_{(r,-s)^D,(r,-s)^D}}$.

One can expect that all the states X in the Potts spectrum (3.5), such that $C^{(1,3)^D}_{X,X} \neq 0$ contribute to $\left\langle V_{(1,3)^D} \right\rangle_\tau$. However, one has to pay special attention, in particular when using truncations in the s-channel spectrum: there can be highly non-trivial cancellations between states. This is known to be the case when the central charge takes rational values, and a finite number of states in the spectrum closes under OPE (see section 5 of [35] and references therein).

We obtain:

$$\left\langle V_{(1,3)^D} \right\rangle_\tau = \frac{1}{Z_Q}\Big((Q-1) C^{(1,3)^D}_{(0,\frac{1}{2}),(0,\frac{1}{2})} \left| \mathcal{F}^{\Delta_{(0,\frac{1}{2})}}_{\Delta_{(1,3)}}(q) \right|^2 + C^{(1,3)^D}_{(1,2)^D,(1,2)^D} \left| \mathcal{F}^{\Delta_{(1,2)}}_{\Delta_{(1,3)}}(q) \right|^2$$
$$+ (Q-1) C^{(1,3)^D}_{(0,\frac{3}{2}),(0,\frac{3}{2})} \left| \mathcal{F}^{\Delta_{(0,\frac{3}{2})}}_{\Delta_{(1,3)}}(q) \right|^2 + \frac{Q(Q-3)}{2} C^{(1,3)^D}_{(2,0),(2,0)} \left| \mathcal{F}^{\Delta_{(2,0)}}_{\Delta_{(1,3)}}(q) \right|^2 + \cdots \Big), \tag{4.25}$$

where $\cdots$ indicates next sub-leading contributions. In the above formula, the Q dependent prefactors come again from the multiplicity of the states propagating in the torus. In the following figure, the value $c_{(1,3)}$ in (4.22) for $M = N$ is plotted as a function of Q in the region of Q where the comparison with Monte Carlo results is possible:

In figure 3 we tagged the values of Q at which Monte Carlo data have been taken.

At $Q = 3$, only three channels ($\mathcal{S}_{\text{int}} = \{(0, \frac{1}{2}), (1,2)^D, (1,3)^D\}$) contribute to $\left\langle V^D_{(1,3)}(0) \right\rangle_\tau$, so we expect that, for $Q \sim 3$, $\{(0, \frac{1}{2}), (1,2)^D\}$ produce the main contributions, while all others are suppressed by some power of $Q - 3$.

5. Monte Carlo simulation and CFT comparisons

5.1. General results for the two-point correlation functions

We collected data on square lattices of size $N \times N$ with periodic boundary conditions on both directions, thus having the topology of a torus (2.14) with $M = N$ (for $M \neq N$ see next subsection). We considered various linear sizes N up to $N = 8192$. The probability (3.6) is computed by considering the lattice points (x, y) and $(x + r, y)$ or (x, y) and $(x, y + r)$ and next averaging over x and y. We took data for $Q = 1 + n/4$ for $n = 1, \cdots 9$ and $Q = 2 + 2\cos\frac{3\pi}{5}, 2 + \sqrt{2}$. For each value of Q, we averaged over 10^6 independent samples generated with the Chayes–Machta algorithm [36, 37]. This algorithm is a generalisation of the Swendsen–Wang algorithm for non integer values of Q.

In figure 4, we present the rescaled correlation function $r^{4\Delta_{(0,\frac{1}{2})}} p_{12}(r)$ as a function of r for various values of Q as shown in the caption. While we observe a plateau for a

J. Stat. Mech. (2020) 023101

value $\simeq 0.7$, we also see that there exist strong deviations for large r. This is due to the fact that we work on a torus, thus we expect topological corrections which have a maximum at $r = \frac{N}{2}$. We also need to take into account the small size corrections which, as can be observed in figure 4, will be present only for small sizes up to $r \simeq 10$. A general form of fit for the rescaled function $r^{4\Delta_{(0,\frac{1}{2})}} p_{12}(r)$ is given by :

$$f(N,r) = c_0 \left(1 + \sum_{j \geqslant 1} c_j \left(\frac{r}{N}\right)^{d_j}\right) \left(1 + g_1\, r^{-g_2}\right) \ . \tag{5.1}$$

The above form of fit is factorised into three factors. The first factor c_0 is the non-universal normalisation of the lattice two-point functions. The second part, with parameters c_j, $(j \geqslant 1)$ encodes the torus corrections: d_j and c_j are the universal quantities to be compared respectively to the dimensions and the factors computed in the previous sections using CFT, see (4.4). The third factor takes into account the small size corrections. In the case of the Ising model, an exact computation shows that this correction is described by this form with $g_2 = 2$ and a small coefficient $g_1 = \frac{1}{64}$ [38].

A first numerical result is that the dominant topological correction is of the form $\left(\frac{r}{N}\right)^{2\Delta_{(1,2)}}$, i.e. $d_1 \sim 2\Delta_{(1,2)}$. In figure 5, we show the behaviour of $r^{4\Delta_{(0,\frac{1}{2})}} p_{12}(r) - c_0$ with c_0 the constant part corresponding to the value of the plateau and this for various values of $Q = 1, \cdots 3$ as shown in the caption and for $N = 8192$. We observe that the correction is a power of r. We do a fit in the range $r \in [50\text{–}200]$ obtaining the powers $d_1 = \{1.251, 1.115, 0.997, 0.898, 0.793\}$ for $Q \in [1,3]$, which are very close to the corresponding set of values of $2\Delta_{(1,2)} = \{1.25, 1.1776, 1, 0.8982, 0.8\}$. The best fit is also shown in figure 5 as thin lines. Note that these fits agree with the numerical data also for much larger distances, $r > 200$. In the case of $Q = 2$, the exact result for the two-point function [27] is :

$$Q = 2, \quad r^2 \left\langle V_{(0,\frac{1}{2})}(r) V_{(0,\frac{1}{2})}(0) \right\rangle_{\tau = i} = 1 + 0.488\,863\, \frac{r}{N} + 0.211\,556\, \left(\frac{r}{N}\right)^4 + \cdots . \tag{5.2}$$

This explains that the leading correction alone gives already a very good fit as shown in figure 5. We observe that this is also true for other values of Q, in agreement with our results (4.4) for $N = M$.

In table 1, we give the numerical results for c_0 and c_1 obtained with a fit while keeping only the leading topological correction and fixing $d_1 = 2\Delta_{(1,2)}$. The fit is done with numerical data $r \in [6, 2048]$. With this range of data, we obtain a good fit (measured with the goodness of fit) for each value of Q. The numerical errors on c_0 and c_1 are indicated in the table either in parenthesis or smaller than one last digit. These fits also take into account small distance corrections. We obtained $g_1 \simeq 0.02$ and $g_2 \simeq 2$ for not too large values of Q. Further details on these fits are found in [20]. In table 1, we also show in the last column the values $c_{(1,2)}$ computed in section 4.2. The agreement is excellent with the numerical value c_1, in particular for small values of Q. For large values of Q, we expect that larger corrections have to be taken into account. In order to check the presence of larger corrections we can simply attempt a fit to the form (5.1) while adding a second correction $c_2 (r/N)^{d_2}$. We will come back to this point later.

J. Stat. Mech. (2020) 023101

5.2. Non-square torus

In this section we extend our results to non-square lattices. We checked the agreement between analytical and numerical results for various aspect ratios $\frac{M}{N}$ and for different Q's. Here we present results for $\frac{M}{N}=2$ and $Q=1$, which involves taking a non-trivial limit, see section 4.1. In this regime, the topological correction coming from the stress-energy tensor is non-zero and is given by (4.10). We consider the correlation measured in the vertical (v) (resp. horizontal (h)) directions. The coefficients $c_T^{(v)}$, $c_T^{(h)}$ of $\left(\frac{r}{N}\right)^2$ (resp. $\left(\frac{r}{M}\right)^2$) and $c_{(1,2)}^{(v)}$, $c_{(1,2)}^{(h)}$ of $\left(\frac{r}{N}\right)^{2\Delta_{(1,2)}}$ (resp. $\left(\frac{r}{M}\right)^{2\Delta_{(1,2)}}$) are,

$$c_T^{(v)} = 2\,c_T(\frac{M}{N}) = 0.175\,608 \quad c_T^{(h)} = 2\left(\frac{M}{N}\right)^{-2} c_T(\frac{N}{M}) = -0.175\,608$$
$$c_{(1,2)}^{(v)} = c_{(1,2)}(\frac{M}{N}) = 0.185\,569 \quad c_{(1,2)}^{(h)} = \left(\frac{M}{N}\right)^{-2\Delta_{(1,2)}} c_{(1,2)}(\frac{N}{M}) = 0.185\,557.$$

In figure 6 we show the numerical results and the best fits (dashed lines). We obtain

$$c_T^{(h)} = -0.165(2) \quad c_T^{(v)} = 0.192(2)$$
$$c_{(1,2)}^{(h)} = 0.183(1) \quad c_{(1,2)}^{(v)} = 0.180(4).$$

The agreement is good. We also show in the inset the difference between vertical and horizontal correlations. This measures directly the contribution of the stress-energy tensor since the contribution of the energy cancels. We obtain $c_T^{(v-h)} = 0.172(1)$.

5.3. Link with one-point correlation function

We compare now the value of c_1 and the theoretical prediction $c_{(1,2)}$ in (4.12) to the torus one-point function of the lattice energy field $\left\langle \varepsilon^{\text{latt}} \right\rangle_\tau$. The lattice energy field can be written in terms of the fields in the thermal series $\mathcal{S}^{D,\text{quot}}_{(1,\mathbb{N}^*)}$, see section 3, giving:

$$\left\langle \varepsilon^{\text{latt}} \right\rangle_\tau = e_0 + \frac{1}{N^{2\,\Delta_{(1,2)}}}\, e_1 + \cdots \tag{5.3}$$

where e_0 is the usual bulk energy density, associated to the identity $V_{(1,1)^D}$ field, and the sub-leading term e_1 is related to the energy $V_{(1,2)^D}$ field:

$$e_1 = (2\pi)^{2\Delta_{(0,\frac{1}{2})}}\, N_\varepsilon^{-1}\, \left\langle V_{(1,2)^D} \right\rangle_\tau . \tag{5.4}$$

In the above formula, N_ε is the normalisation relating the lattice to the scaling energy field and is computed by determining the energy-energy correlation $\left\langle \varepsilon^{\text{latt}}(x)\varepsilon^{\text{latt}}(0) \right\rangle_\tau$, in a similar way as we evaluate c_0 for the connectivity function.

In practice, we define the energy operator $\varepsilon^{\text{latt}}(x)$ as the probability that it contains a FK bond. For a given cluster configuration, $b_o(x)$ is the probability that the site $x=(x_1,x_2)$ is in the same FK cluster as the site (x_1+1,x_2) and $b_v(x)$ is the probability that the site x is in the same FK cluster as the site (x_1,x_2+1). Then the energy operator is defined as

$$\varepsilon^{\text{latt}}(x) = b_o(x) + b_v(x) - 1. \tag{5.5}$$

J. Stat. Mech. (2020) 023101

Table 2. Comparison of the dimensions of the fourh descendant of the energy, and of the field $V_{(1,3)}$, and thus of the sub-dominants $\frac{r}{N}$ corrections, for different values of Q.

Q	$2\Delta_{(1,2)}+4$	$2\Delta_{(1,3)}$
1	5.25	4
2	5	3.33
3	4.8	2.8

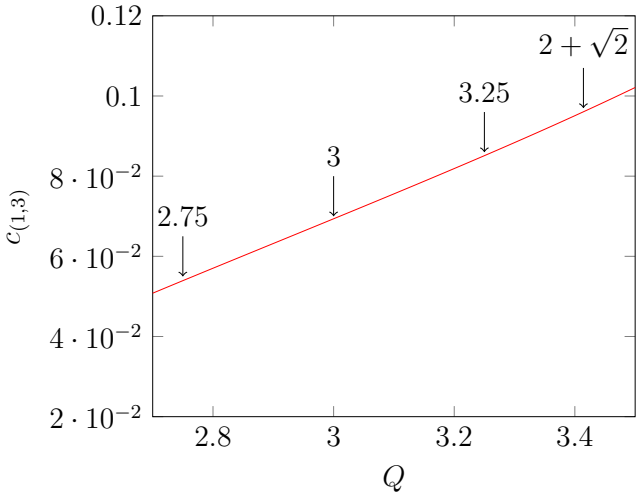

Figure 3. The coefficient $c_{(1,3)}$, computed for values of Q close to 3, where it produces a visible contribution. We tagged the values of Q at which Monte Carlo data has been taken.

This subtraction corresponds to imposing $e_0 = 0$ in (5.3). e_1 is obtained by measuring $\left\langle \varepsilon^{\text{latt}} \right\rangle_\tau$ and fitting to the form (5.3). The constant N_ε is fixed by measuring the two-point energy operator. The measurement for the one-point correlation function have been done on small lattices, up to $N = 256$ for the computation of e_1 and with 100 million samples for each size. We need to use many samples (and then not too big lattices), since $2\Delta_{(1,2)} = O(1)$ and then the deviation from the infinite size is very small. The same is also true for N_ε: it is determined from the two-point energy function which decreases very quickly as a function of the distance. The fits were done for distances $r = 8$–30 where we ignored small size and topological corrections. As a comparison, the measurements for c_1 from the two-point correlation function have been done on very large lattices, $N = 8192$. In figure 7, we compare the result $C^{(1,2)^D}_{(0,\frac{1}{2}),(0,\frac{1}{2})}\, N_\varepsilon\, e_1$ (shown in green) with c_1 computed numerically (shown as red circles) and with $c_{(1,2)}$ of (4.12) (shown as blue circles). The agreement between the two measured quantities and the analytical result is very good.

In the limit $Q \to 1$, we observe that $C^{(1,2)^D}_{(0,\frac{1}{2}),(0,\frac{1}{2})}\, N_\varepsilon\, e_1$ converges to the measured value c_1 and $c_{(1,2)}$. Indeed, we can check numerically that, for $Q \simeq 1$, one has $e_1 \simeq 0.25\ (Q-1)$ while $N_\epsilon \simeq 5.0\ (Q-1)^{-0.5}$.

https://doi.org/10.1088/1742-5468/ab6331

J. Stat. Mech. (2020) 023101

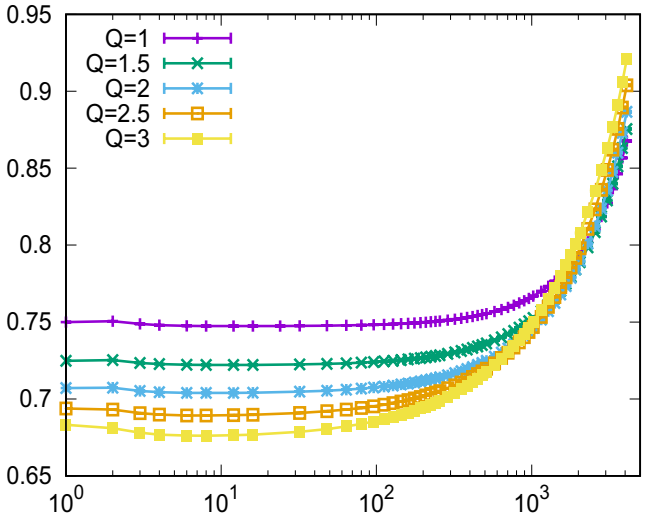

Figure 4. Rescaled two-point connectivity for the Q Potts models at $N = 8192$ for various values of Q as shown in the caption.

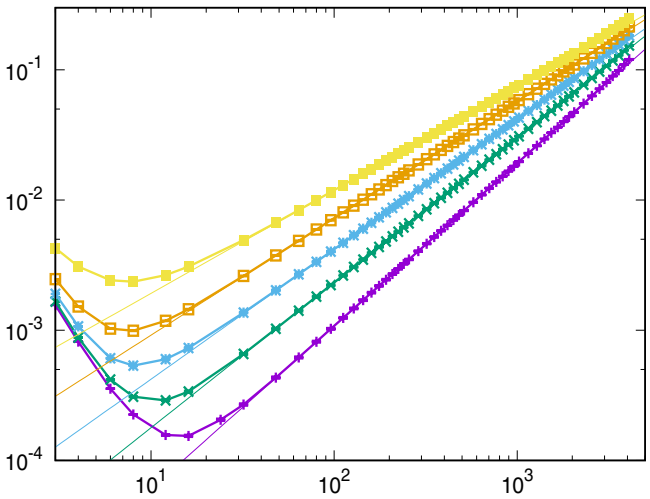

Figure 5. Same data as in figure 4 with the subtraction of the plateau. The thin lines corresponds to best fit as discussed in the text.

5.4. Further corrections

We want to check numerically the existence of further topological corrections. We expect that there exist corrections of order 4 from the descendants of the identity, see section 4.1 and of order $2\Delta_{(1,2)} + 4$ from the energy descendants, see section 4.2. There exist also the contribution of order $2\Delta_{(1,3)}$, see section 4.3. In table 2 we give a comparison of their respective dimensions.

For $Q < 3$ the coefficient $c_{(1,3)}$ becomes very small (see figure 3 in section 4.3), while the dimension $2\Delta_{(1,3)}$ is large and comparable to the dimensions of the descendant fields. Numerically it will then be difficult to distinguish the different contributions for small Q's.

We first compare our numerical data to a fit of the form

$$f(N, r) = c_0 \left(1 + c_1 \left(\frac{r}{N}\right)^{d_1} + c_2 \left(\frac{r}{N}\right)^{d_2}\right) (1 + g_1 r^{-g_2}) \,. \tag{5.6}$$

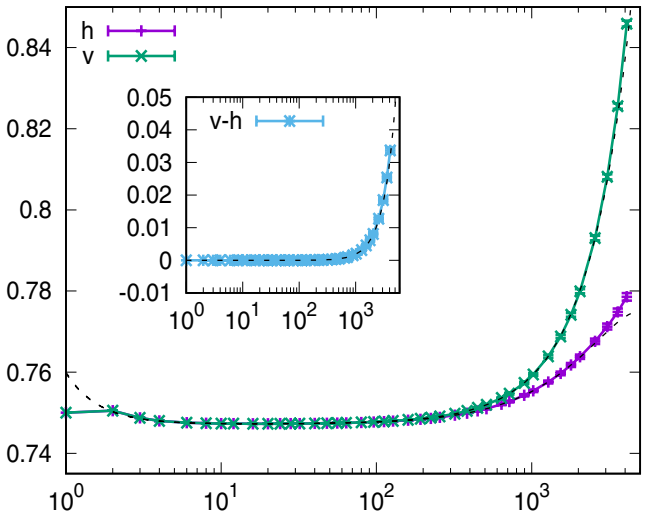

Figure 6. Rescaled two-point connectivity for $Q = 1$ and $\frac{M}{N} = 2$, at $N = 8192$. We show separately the vertical and horizontal connectivities. The inset contains the difference between these two connectivities.

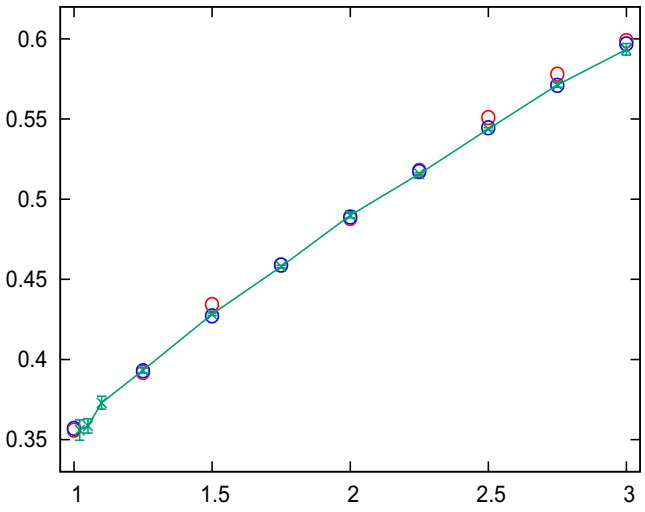

Figure 7. $C^{(1,2)^D}_{(0,\frac{1}{2}),(0,\frac{1}{2})} N_\varepsilon e_1$ versus Q compared to the numerical values c_1 shown as red circles and the analytical predictions $c_{(1,2)}$ shown as blue circles.

Here d_2 is an effective dimension which takes into account all possible higher corrections, while we assume the value $d_1 = 2\Delta_{(1,2)}$ and we take for $c_1 = c_{(1,2)}$, see (4.12). Even so, it is a difficult task since we are left with five parameters. One could try to ignore the small distance corrections by considering only data at large distances, say $r > r_{\min} = 50$. This is what we have done for determining the power corresponding to the dominant correction. We consider a fit in the range $r_{\min} \leqslant r \leqslant r_{\max}$, with $r_{\min} = 50$ and $r_{\max} = 4096$. For the second correction, the fit gives a much less clear image. We observe that the second correction is much larger than $d_1 = 2\Delta_{(1,2)}$ and its value decreases with Q. We measure $c_2 \simeq 0.44$ and $d_2 \simeq 5.3$ for $Q = 1$; $c_2 \simeq 0.35$ and $d_2 \simeq 4.4$ for $Q = 2$; $c_2 \simeq 0.29$ and $d_2 \simeq 3.6$ for $Q = 3$. We only quote approximate numbers for c_2 and d_2 since they depend on the range $r_{\min}$ and $r_{\max}$. Still we observe that only for

large values of Q, i.e. $Q \simeq 3$, we have a dimension $d_2 < 4$. This is in agreement with what we expect since it is only for Q close to 3 that the exponent $2\Delta_{(1,3)}$ is smaller than 4 and $c_{(1,3)}$ becomes non negligible. For smaller values of Q, our numerics are not able to give further information.

For $Q = 3$, we can improve by trying a fit to the form

$$f(N,r) = c_0 \left(1 + c_1 \left(\frac{r}{N}\right)^{d_1} + c_2 \left(\frac{r}{N}\right)^{d_2} + c_3 \left(\frac{r}{N}\right)^{d_3}\right) \left(1 + g_1\, r^{-g_2}\right) , \qquad (5.7)$$

while imposing the dimensions $d_1 = 2\Delta_{(1,2)}$, $d_2 = 2\Delta_{(1,3)}$ and $d_3 = 4$ or $2\Delta_{(1,2)} + 4$. In a fit with $r \geqslant 50$, we obtain a value of c_2 in the range $0.05 - 0.08$ (the smallest value is obtained for $d_3 = 4$ and the largest for $d_3 = 2\Delta_{(1,2)} + 4 = 4.8$), that is comparable with the prediction $c_{(1,3)} \simeq 0.07$ given by (4.22) for $Q = 3$ (see figure 3).

6. Conclusions

In this paper we considered the two-point connectivity p_{12} (3.6) of the critical Q-random cluster Potts model (3.1) on a torus of parameters (2.14). We focused on the universal corrections to the plane scaling limit of p_{12} originating from the torus topology for general values of $Q \in [1, 4]$. Combining CFT techniques with Monte Carlo insights, which suggested the ansatz (4.1), we have computed analytically the first dominant corrections to p_{12} in the limit (4.2). The theoretical results on p_{12}, summarised in (4.4), found a very good agreement with Monte Carlo measurements, as shown in figure 5 and in table 1. Moreover, we tested the CFT one-point torus energy function (4.15) against Monte Carlo measurements of the corresponding lattice observable, obtaining again a very good agreement, as shown in figure 7.

Our theoretical results probe non trivial features of the CFT describing the Q-state random Potts model, such as the multiplicities of the spectrum (3.5) or the validity of the three-point functions (4.16) and (4.24) for general values of the central charge. The topological corrections furnish a subtle characterisation of the Potts random clusters which goes beyond the computation of their fractal dimension. As a special case, we obtained the result (4.5) that represents a new universal behaviour of critical percolation. The study of the torus two-point connectivity represents, together with the plane three-point connectivity [39], a natural and powerful method to test various conjectures related to critical percolation.

Acknowledgments

We are grateful to Vladimir Dotsenko, Benoit Estienne, Christian Hagendorf, Yacine Ikhlef, Jesper Jacobsen, for helpful discussions and we thank in particular Sylvain Ribault with whom this project started.

Appendix. The *s*-channel expansion of the torus two-point function

The Virasoro generators are the modes of the stress-energy tensor. On the plane $z \in \mathbb{C} \bigcup \{\infty\}$, they are defined as:

J. Stat. Mech. (2020) 023101

$$L_n^{(z)} V_{(\Delta,Y)}(z,\bar{z}) = \frac{1}{2\pi \mathrm{i}} \oint_{\mathcal{C}_z} \mathrm{d}\, z'\, (z'-z)^{n+1}\, T(z') V_{(\Delta,Y)}(z,\bar{z}), \quad n \in \mathbb{Z}. \tag{A.1}$$

Under a conformal map $z' = f(z)$, a primary operator transforms:

$$V_{(\Delta)}(z,\bar{z}) = f'(z)^{\Delta} \bar{f}'(\bar{z})^{\bar{\Delta}}\, V_{(\Delta)}(f(z), \bar{f}(\bar{z})), \tag{A.2}$$

while the transformation of the Virasoro generators takes the form [24][3]:

$$\begin{aligned} L_n^{(z)} &= \frac{c}{12}\frac{1}{2\pi \mathrm{i}} \oint_z \mathrm{d}y (y-z)^{n+1} \{f, y\} + \frac{1}{2\pi \mathrm{i}} \oint_z \mathrm{d}y \sum_m \frac{L_m^{(f(z))} [f'(y)]^2}{(f(y)-f(z))^{m+2}} (y-z)^{n+1} \\ &= \frac{c}{12}\frac{1}{2\pi \mathrm{i}} \oint_z \mathrm{d}y (y-z)^{n+1} \{f, y\} + [f'(z)]^{-n} L_n^{(f(z))} + \frac{1-n}{2} f'' (f')^{-n-2} L_{n+1}^{(f(z))} \\ &\quad + \left(\frac{2-n}{6} f' f''' + \frac{1}{8}(n^2+n-4)(f'')^2\right)(f')^{-n-4} L_{n+2}^{(f(z))} + \cdots \end{aligned} \tag{A.3}$$

where $\{f, y\}$ is the Schwarzian derivative.

To compute torus correlation functions, one needs to know the transformation of (A.1) under the map (2.15). For finite w, one obtains for instance:

$$\begin{aligned} L_0^{(z)} &= L_0^{\mathcal{C},(w)} \\ L_{-1}^{(z)} &= z^{-1} \left(\frac{N}{2\pi \mathrm{i}}\right) \left(L_{-1}^{\mathcal{C},(w)} - \frac{2\pi \mathrm{i}}{N} L_0^{\mathcal{C},(w)}\right) \\ L_{-2}^{(z)} &= z^{-2} \left(\frac{N}{2\pi \mathrm{i}}\right)^2 \left(L_{-2}^{\mathcal{C},(w)} - \frac{3}{2}\frac{2\pi \mathrm{i}}{N} L_{-1}^{\mathcal{C},(w)} + \frac{13}{12}\left(\frac{2\pi \mathrm{i}}{N}\right)^2 L_0^{\mathcal{C},(w)} + \left(\frac{2\pi \mathrm{i}}{N}\right)^2 \frac{c}{24}\right) \\ &\cdots \end{aligned} \tag{A.4}$$

The modes with $L_n^{\mathcal{C},(w=\infty)}$, obtained from $L_n^{(0)}$ are instead related to contour integrals that are non-contractible on the cylinder. One finds for instance:

$$L_{-n}^{(0)} = L_{-n}^{\mathcal{C},(\infty)} + \frac{c}{24}\delta_{n,0}. \tag{A.5}$$

Using the above relation, one can easily verify that the one-point torus function of total derivative $\langle L_{-1}^{\mathcal{C},(0)} V_{(\Delta)} \rangle_\tau \propto \langle (L_{-1}^{(1)} + L_0^{(1)}) V_{(\Delta)} \rangle$ vanishes, as can be seen from the vanishing of the matrix elements (2.8):

$$\begin{aligned} &\left\langle L_{Y'}^{(\infty)} V_{(\Delta')} L_{-1}^{(1)} V_{(\Delta)} L_{-Y}^{(0)} V_{(\Delta')} \right\rangle + \left\langle L_{Y'}^{(\infty)} V_{(\Delta')} L_0^{(1)} V_{(\Delta)} L_{-Y}^{(0)} V_{(\Delta')} \right\rangle \\ &\qquad = (|Y| - |Y'| - \Delta + \Delta) \left\langle L_{Y'}^{(\infty)} V_{(\Delta')} V_{(\Delta)} L_{-Y}^{(0)} V_{(\Delta')} \right\rangle = 0. \end{aligned} \tag{A.6}$$

For the two-point function one obtains using (2.15):

$$\langle V_{(\Delta_1)}(w_1,\bar{w}_1) V_{(\Delta_2)}(w_2,\bar{w}_2) \rangle_\tau = \frac{1}{Z} \mathrm{Tr}_{\mathcal{S}_{\mathrm{int}}} \left(q^{L_0^{\mathcal{C},(\infty)}} \bar{q}^{\bar{L}_0^{\mathcal{C},(\infty)}} V_{(\Delta_1)}(w_1,\bar{w}_1) V_{(\Delta_2)}(w_2,\bar{w}_2) \right). \tag{A.7}$$

Using (A.2) under the map (2.15)[4] and the OPE (2.5), we find:

[3] Note that there is a misprint in [24] for the term $m = n+2$, as can be checked explicitly in the case $f(z) = z^2$.
[4] Note that the is drop since the dimensions of our fields satisfy $\Delta - \bar{\Delta} \in 2\mathbb{Z}$.

J. Stat. Mech. (2020) 023101

$$V_{(\Delta_1)}(w_1,\bar{w}_1)V_{(\Delta_2)}(w_2,\bar{w}_2) = \left(\frac{2\pi}{N}\right)^{\Delta_1+\Delta_2}\left(\frac{2\pi}{N}\right)^{\bar{\Delta}_1+\bar{\Delta}_2} z_1^{\Delta_1}z_2^{\Delta_2}\bar{z}_1^{\bar{\Delta}_1}\bar{z}_2^{\bar{\Delta}_2}V_{(\Delta_1)}(z_1,\bar{z}_1)V_{(\Delta_2)}(z_2,\bar{z}_2)$$
$$= \left(\frac{2\pi}{N}\right)^{\Delta_1+\Delta_2}\left(\frac{2\pi}{N}\right)^{\bar{\Delta}_1+\bar{\Delta}_2} z_1^{\Delta_1}z_2^{\Delta_2}\bar{z}_1^{\bar{\Delta}_1}\bar{z}_2^{\bar{\Delta}_2}$$
$$\times \sum_{(\Delta,Y)} C^{(\Delta)}_{(\Delta)_1,(\Delta)_2} z_{12}^{-\Delta_1-\Delta_2+\Delta+Y}\bar{z}_{12}^{-\bar{\Delta}_1-\bar{\Delta}_2+\bar{\Delta}+\bar{Y}}\tilde{\beta}^{(\Delta,Y)}_{\Delta_1,\Delta_2}\tilde{\beta}^{(\bar{\Delta},\bar{Y})}_{\bar{\Delta}_1,\bar{\Delta}_2}V_{(\Delta,Y)}(z_2,\bar{z}_2) \tag{A.8}$$

where we made explicit the z dependence of the coefficients (2.7): $\beta^{(\Delta,Y)}_{\Delta_1,\Delta_2}(z_{12}) = z_{12}^{-\Delta_1-\Delta_2+\Delta+Y}\tilde{\beta}^{(\Delta,Y)}_{\Delta_1,\Delta_2}$. Mapping $V_{(\Delta,Y)}(z_2,\bar{z}_2)$ back to the cylinder:

$$V_{(\Delta,Y)}(z_2,\bar{z}_2) = \left(\frac{2\pi\mathrm{i}}{N}\right)^{-\Delta-Y} z_2^{-\Delta-Y}\left(-\frac{2\pi\mathrm{i}}{N}\right)^{-\bar{\Delta}-\bar{Y}}\bar{z}_2^{-\bar{\Delta}-\bar{Y}}\left(L^{\mathcal{C},w_2}_{-Y}+\cdots\right)\left(\bar{L}^{\mathcal{C},\bar{w}_2}_{-\bar{Y}}+\cdots\right)V^{\mathcal{C}}_{(\Delta)}(w_2,\bar{w}_2)$$

where $\left(L^{\mathcal{C},w_2}_{-Y}+\cdots\right)$ is a linear combination of generators on the cylinder as in relations (A.4). We can now take the trace, and writing only the holomorphic part we get:

$$\langle V_{(\Delta_1)}(w_1)V_{(\Delta_2)}(w_2)\rangle_\tau = \left(\frac{2\pi}{N}\right)^{\Delta_1+\Delta_2}\left(\frac{z_2}{z_1}\right)^{\Delta_2}\left(1-\frac{z_2}{z_1}\right)^{-\Delta_1-\Delta_2}$$
$$\times \sum_{(\Delta,Y)\in\mathcal{S}_{\mathrm{int}}} C^{(\Delta)}_{(\Delta)_1,(\Delta)_2}\tilde{\beta}^{(\Delta,Y)}_{\Delta_1,\Delta_2}\left(\frac{2\pi\mathrm{i}}{N}\right)^{-\Delta-Y}\left(\frac{z_2}{z_1}\right)^{-\Delta-Y}\left(1-\frac{z_2}{z_1}\right)^{\Delta+Y}\langle\left(L^{\mathcal{C},w_2}_{-Y}+\cdots\right)V^{\mathcal{C}}_{(\Delta)}(w_2)\rangle_\tau. \tag{A.9}$$

Writing $\frac{z_2}{z_1} = \mathrm{e}^{-\frac{2\pi\mathrm{i}}{N}w_{12}}$ and expanding the exponentials, one has:

$$\begin{aligned}\langle V_{(\Delta_1)}(w_1)V_{(\Delta_2)}(w_2)\rangle_\tau &= w_{12}^{-\Delta_1-\Delta_2}\sum_{(\Delta)\in\mathcal{S}_{\mathrm{int}}} w_{12}^{\Delta}C^{(\Delta)}_{(\Delta)_1,(\Delta)_2}\Bigg(\langle V_{(\Delta)}(w_2)\rangle_\tau \\ &\quad + w_{12}\left\{\frac{2\pi\mathrm{i}}{N}\frac{\Delta_1-\Delta_2+\Delta}{2}+\tilde{\beta}^{(\Delta,1)}_{\Delta_1,\Delta_2}(L^{\mathcal{C},(w_2)}_{-1}-\frac{2\pi\mathrm{i}}{N}L^{\mathcal{C},(w_2)}_0)\right\}\langle V_{(\Delta)}(w_2)\rangle_\tau + O(w_{12}^2)\Bigg) \\ &= w_{12}^{-\Delta_1-\Delta_2}\sum_{(\Delta)\in\mathcal{S}_{\mathrm{int}}} w_{12}^{\Delta}C^{(\Delta)}_{(\Delta)_1,(\Delta)_2}\Bigg(\langle V_{(\Delta)}(w_2)\rangle_\tau \\ &\quad + w_{12}\tilde{\beta}^{(\Delta,1)}_{\Delta_1,\Delta_2}\langle L^{\mathcal{C},(w_2)}_{-1}V_{(\Delta)}(w_2)\rangle_\tau + O(w_{12}^2)\Bigg).\end{aligned} \tag{A.10}$$

We assume that such cancellations occur at every order in w_{12}. Using the notation (2.16), we can finally arrive at equation (2.21). Notice that the coefficients $a^{(\Delta,Y)_{\mathrm{int}}}_{(\Delta)_1,(\Delta)_2}$ are evaluated using the generators on the plane, while the descendant fields $V^{\mathcal{C}}_{(\Delta,Y)}$ are obtained by acting with the cylinder generators.

References

[1] Duplantier B 2006 Conformal random geometry (arXiv:math-ph/0608053)
[2] Bauer M and Bernard D 2006 2D growth processes: SLE and Loewner chains *Phys. Rep.* **432** 115–221
[3] Cardy J L 1992 Critical percolation in finite geometries *J. Phys. A: Math. Gen.* **25** L201
[4] Cardy J 2005 SLE for theoretical physicists *Ann. Phys.* **318** 81–118
[5] Gaberdiel M R and Kausch H G 1999 A local logarithmic conformal field theory *Nuclear Phys.* B **538** 631–58

J. Stat. Mech. (2020) 023101

[6] Kausch H G 2000 Symplectic fermions *Nuclear Phys.* B **583** 513–41
[7] Wu F Y 1982 The Potts model *Rev. Mod. Phys.* **54** 235
[8] Caracciolo S, Jacobsen J L, Saleur H, Sokal A D and Sportiello A 2004 Fermionic field theory for trees and forests *Phys. Rev. Lett.* **93** 080601
[9] Delfino G and Viti J 2011 Potts q-color field theory and scaling random cluster model *Nuclear Phys.* B **852** 149–73
[10] Gori G and Viti J 2017 Exact logarithmic four-point functions in the critical two-dimensional Ising model *Phys. Rev. Lett.* **119** 191601
[11] Gori G and Viti J 2018 Four-point boundary connectivities in critical two-dimensional percolation from conformal invariance *J. High Energy Phys.* **2018** 131
[12] Delfino G and Viti J 2011 On three-point connectivity in two-dimensional percolation *J. Phys. A: Math. Theor.* **44** 032001
[13] Picco M, Santachiara R, Viti J and Delfino G 2013 Connectivities of Potts Fortuin–Kasteleyn clusters and time-like Liouville correlator *Nuclear Phys.* B **875** 719–37
[14] Delfino G, Picco M, Santachiara R and Viti J 2013 Spin clusters and conformal field theory *J. Stat. Mech.* P11011
[15] Estienne B and Ikhlef Y 2015 Correlation functions in loop models (arXiv:1505.00585)
[16] Ikhlef Y, Lykke Jacobsen J and Saleur H 2015 Three-point functions in $c \leqslant= 1$ Liouville theory and conformal loop ensembles *Phys. Rev. Lett.* **116** 130601
[17] LeClair A and Squires J 2018 Conformal bootstrap for percolation and polymers *J. Stat. Mech.* 123105
[18] Jacobsen J L and Saleur H 2018 Bootstrap approach to geometrical four-point functions in the two-dimensional critical Q-state Potts model: a study of the s-channel spectra (arXiv:1809.02191)
[19] Picco M, Ribault S and Santachiara R 2016 A conformal bootstrap approach to critical percolation in two dimensions *SciPost Phys.* **1** 009
[20] Picco M, Ribault S and Santachiara R 2019 On four-point connectivities in the critical 2d Potts model *SciPost Phys.* **7** 044
[21] Ribault S 2014 Conformal field theory on the plane (arXiv:1406.4290)
[22] Ribault S and Santachiara R 2015 Liouville theory with a central charge less than one *J. High Energy Phys.* 109
[23] Kanno S, Matsuo Y and Shiba S 2010 Analysis of correlation functions in Toda theory and AGT-W relation for SU(3) quiver *Phys. Rev.* D **82** 066009
[24] Eguchi T and Ooguri H 1987 Conformal and current algebras on a general Riemann surface *Nuclear Phys.* B **282** 308–28
[25] Javerzat N, Santachiara R and Foda O 2018 Notes on the solutions of Zamolodchikov-type recursion relations in Virasoro minimal models *J. High Energy Phys.* 109
[26] Fortuin C and Kasteleyn P 1972 On the random-cluster model: I. Introduction and relation to other models **57** 536–64
[27] Di Francesco P, Saleur H and Zuber J-B 1987 Relations between the Coulomb gas picture and conformal invariance of two-dimensional critical models *J. Stat. Phys.* **49** 57–79
[28] Dotsenko V and Fateev V 1985 Operator algebra of two-dimensional conformal theories with central charge $C \leqslant 1$ *Phys. Lett.* B **154** 291–5
[29] Jacobsen J 2012 Loop models and boundary CFT Henkel M and Karevski D *Conformal Invariance: an Introduction to Loops, Interfaces and Stochastic Loewner Evolution* (Berlin: Springer)
[30] Saleur H 1987 Conformal invariance for polymers and percolation *J. Phys. A: Math. Gen.* **20** 455
[31] Beffara V and Duminil-Copin H 2010 The self-dual point of the two-dimensional random-cluster model is critical for $q \geqslant 1$ (arXiv:1006.5073)
[32] Jayaraman T and Narain K 1990 Correlation functions for minimal models on the torus *Nuclear Phys.* B **331** 629–58
[33] Dotsenko V and Fateev V 1985 Four-point correlation functions and the operator algebra in 2D conformal invariant theories with central charge $C \leqslant 1$ *Nuclear Phys.* B **251** 691–734
[34] Migliaccio S and Ribault S 2017 The analytic bootstrap equations of non-diagonal two-dimensional CFT *J. High Energy Phys.* 169
[35] Santachiara R and Viti J 2014 Local logarithmic correlators as limits of Coulomb gas integrals *Nuclear Phys.* B **882** 229–62
[36] Chayes L and Machta J 1998 Graphical representations and cluster algorithms II *Physica* A **254** 477–516
[37] Deng Y, Garoni T M, Machta J, Ossola G, Polin M and Sokal A D 2007 Dynamic critical behavior of the Chayes–Machta algorithm for the random-cluster model, I. two dimensions *J. Stat. Phys.* **144** 459
[38] Wu T T, McCoy B M, Tracy C A and Barouch E 1976 Spin-spin correlation functions for the two-dimensional Ising model: exact theory in the scaling region *Phys. Rev.* B **13** 316
[39] Cao X, Rosso A and Santachiara R 2015 Conformal invariance of loop ensembles under Kardar–Parisi–Zhang dynamics *EPL* **111** 16001

J. Stat. Mech. (2020) 023101